Biosensors and Bioelectronics 100 (2018) 437–444

Contents lists available at ScienceDirect

Biosensors and Bioelectronics

journal homepage: www.elsevier.com/locate/bios

Lipidic liquid crystalline cubic phases for preparation of ATP-hydrolysing enzyme electrodes

Martina Zatloukalová[a,b], Ewa Nazaruk[a], David Novák[b], Jan Vacek[b,*], Renata Bilewicz[a,*]

[a] Faculty of Chemistry, University of Warsaw, Pasteura 1, 02-093 Warsaw, Poland
[b] Department of Medical Chemistry and Biochemistry, Faculty of Medicine and Dentistry, Palacký University, Hněvotínská 3, 775 15 Olomouc, Czech Republic

ARTICLE INFO

Keywords:
Lipid cubic phase
Sodium potassium pump
Enzyme activity
Protein biosensor
Voltammetry
ATPase

ABSTRACT

The lipidic liquid-crystalline cubic phase (LCP) is a membrane-mimetic material useful for the stabilization and structural analysis of membrane proteins. Here, we focused on the incorporation of the membrane ATP-hydrolysing sodium/potassium transporter Na^+/K^+-ATPase (NKA) into a monoolein-derived LCP. Small-angle X-ray scattering was employed for the determination of the LCP structure, which was of Pn3m symmetry for all the formulations studied. The fully characterized NKA-LCP material was immobilized onto a glassy carbon electrode, forming a highly stable enzyme electrode and a novel sensing platform. A typical NKA voltammetric signature was monitored *via* the anodic reaction of tyrosine and tryptophan residues. The *in situ* enzyme activity evaluation was based on the ability of NKA to transform ATP to ADP and free phosphate, the latter reacting with ammonium molybdate to form the ammonium phosphomolybdate complex under acidic conditions. The square-wave voltammetric detection of phosphomolybdate was performed and complemented with spectrophotometric measurement at 710 nm. The anodic voltammetric response, corresponding to the catalytic ATP-hydrolysing function of NKA incorporated into the LCP, was monitored at around + 0.2 V *vs.* Ag/AgCl in the presence or absence of ouabain, a specific NKA inhibitor. NKA incorporated into the LCP retained its ATP-hydrolysing activity for 7 days, while the solubilized protein became practically inactive. The novelty of this work is the first incorporation of NKA into a lipidic cubic phase with consequent enzyme functionality and stability evaluation using voltammetric detection. The application of LCPs could also be important in the further development of new membrane protein electrochemical sensors and enzyme electrodes.

1. Introduction

Membrane proteins, located in lipid bilayers, are involved in important cellular processes, such as the transport of ions and low-molecular weight compounds, the conversion of energy, signal transduction, and cell-cell interactions. Understanding these processes at a molecular level requires knowledge of the structure of these proteins and the retention of their activity under the selected experimental conditions. The incorporation or reconstitution of membrane proteins into lipid systems, such as linear lipid monolayers, supported lipid bilayers, liposomes, lipid nanodiscs, or more complex systems such as lipidic cubic phases, enables them to retain their activity and global or local structural integrity. The above point is an important prerequisite for subsequent structural/functional analysis and the investigation of membrane protein biomolecular interactions (Caffrey, 2015; Landau and Luisi, 1993; Landau and Rosenbusch, 1996; Razumas et al., 1994; Van'T Hag et al., 2016; Zabara et al., 2014). From the methodological point of view, current research focuses on the development of stable lipid membrane-mimetic systems and versatile sensing devices and biosensors useful for the characterization and trace analysis of membrane proteins and their lipid membrane associates. This study is devoted to the immobilization of the lipidic liquid crystalline cubic phase (LCP), as a suitable accommodation matrix for the ATP-hydrolysing transmembrane protein sodium-potassium pump, onto a carbon electrode surface. In this way, a functional and highly stable enzyme electrode was developed.

LCPs are suitable materials for protein immobilization, since they are stable in excess water, biocompatible, and can accommodate relatively large loads of host material due to their high surface area of *ca.* 400 $m^2\ g^{-1}$ (Angelov et al., 2003; Kulkarni et al., 2011; Luzzati et al., 1968). Cubic phases are formed upon mixing lipids with water in a certain ratio and generally occur in two different arrangements, the closed discontinuous micellar array and the bicontinuous cubic phase, which exhibits a three-dimensional, continuous membrane bilayer. The structural parameters of LCPs depend on the composition of the aqueous part and on the selected lipid. Frequently used lipids for the

* Corresponding authors.
E-mail addresses: jan.vacek@upol.cz (J. Vacek), bilewicz@chem.uw.edu.pl (R. Bilewicz).

http://dx.doi.org/10.1016/j.bios.2017.09.036
Received 27 May 2017; Received in revised form 17 September 2017; Accepted 18 September 2017
Available online 20 September 2017
0956-5663/

formation of LCPs are monoacylglycerols, specifically 1-monoolein (MO) (Qiu and Caffrey, 2000). The highly structured reverse LCPs, which are composed of curved lipid bilayers surrounded by two identical, non-intersecting aqueous channels, exhibit interesting properties as the host materials of biologically important molecules. Because of their internal structure, LCPs can incorporate hydrophilic, amphiphilic, and hydrophobic drugs, enzymes, and other bioactive molecules of various sizes and molecular weights. LCPs have therefore been investigated as drug carriers (Boyd et al., 2006; Fong et al., 2016; Nazaruk et al., 2015) and as hosting matrices for redox enzymes, while the deposition of these catalytic films on electrode surfaces has also been studied (Nazaruk et al., 2014, 2008; Razumas et al., 1994).

Embedding the transmembrane proteins in the cubic phase has often been used for the crystallization of these proteins (Landau and Rosenbusch, 1996); however, only a few studies have been devoted to their functions and the evaluation of their activity when immobilized in this biocompatible environment. The activity of photosynthetic protein transporters, (Katona et al., 2003) heme-copper oxidases, (Li and Caffrey, 2011) the ion channel KvLm, (Santos et al., 2012) outer membranes proteins, and the enzyme DgaK were also investigated in LCPs (Tiefenbrunn et al., 2011).

Here we present for the first time the cubic phase as a suitable environment for the immobilization of the transmembrane protein sodium-potassium pump in its fully functional form on the electrode surface. The sodium-potassium pump (EC 3.6.3.9), also known as Na^+/K^+-ATPase (NKA), is a transmembrane plasma protein that actively transfers sodium and potassium ions against their electrochemical potential gradients. The energy necessary to transport ions is obtained from the hydrolysis of ATP. During this process, NKA changes structure between two conformation states, E1 and E2. In the E1 state, NKA has a high affinity for sodium ions and ATP; therefore, the channel is opened toward the cytoplasm side. In the E2 state, the cation binding site is oriented towards the extracellular space, and NKA has a high affinity for potassium ions (Kaplan, 2002). Structurally, the sodium potassium pump is a heterodimeric protein, consisting of an α-subunit (109 kDa) and a smaller β-subunit (55 kDa). The α-subunit is responsible for the catalytic function of ATP hydrolysis, and the β-subunit is necessary for the proper maturation of the enzyme in the plasma membrane (Geering, 2001; Toyoshima et al., 2011). Both subunits, together with the gamma unit, are highlighted in the molecular visualization (3WGV) in Scheme 1.

For the evaluation of NKA activity, the transformation of ATP to ADP accompanied by free phosphate (P_i) release is monitored. As previously described, the determination of the release of phosphates can be monitored by spectrophotometry based on the reaction with ammonium molybdate (Bartolommei et al., 2013; Sarkadi et al., 1992), BIOMOL Green reagent (Juel et al., 2013), or Malachite Green (Benabdelhak et al., 2005), or alternatively by using labelled phosphate for liquid scintillation analysis (Dalla et al., 2013; Ferrandi et al., 1996) or fluorimetric methods (Johansson et al., 2000). To the best of our knowledge, the quantitative electrochemical evaluation of NKA's function has not yet been reported.

The aims of our studies were to **(a)** prepare a stable LCP with incorporated NKA enzyme, (b) cover the carbon electrode surface with the NKA-LCP layer, **(c)** evaluate NKA functionality (ATP-hydrolysing activity) *in situ* using the electrochemical monitoring of free phosphate and complement the electrochemical data with spectrophotometric results, and **(d)** estimate the ATP-hydrolysing activity (enzyme stability) of NKA embedded in LCP over a 14-day period.

2. Experimental section

2.1. Reagents

Chemicals were purchased from Sigma Aldrich (St. Louis, MO, USA), BioRad Laboratories (Hercules, CA, USA), or POCh (Polish Chemicals Co.). Monoolein was purchased from Hampton Research (Aliso Viejo, CA, USA). All solutions were prepared using Milli-Q water (18.2 MΩ cm^{-1}), (Millipore, Bedford, MA, USA). The sample preparation and analyses were performed under aerobic conditions.

2.2. Protein isolation, solubiliation, and purification

Two NKA samples, based on different isolation and solubiliation protocols, were used. The first one was commercially available NKA (Sigma-Aldrich), which was solubilized in 50 mM TRIS/HCl buffer (pH 7.4) containing 4.5 mg ml^{-1} octaethylene glycol monododecyl ether ($C_{12}E_8$) detergent (*sample A*). The second one was NKA isolated from fresh pig kidney (donated by Makovec Co., Czech Republic). The method of Klodos et al. (2002) was used for isolation. Briefly, after several homogenization and centrifugation steps on kidney tissue in ISE buffer (25 mM imidazole, 250 mM sucrose, 1 mM ethylenediaminetetraacetic acid, pH 7.4), the corresponding amount of sodium dodecyl sulphate (0.24 mg SDS/mg protein) was used for protein solubiliation (*sample B*).

The protein concentration was determined by Bradford or bicinchoninic acid protein assays (Bradford, 1976). The protein purity was verified by SDS-PAGE carried out on 10% polyacrylamide gels with Coomassie Brilliant Blue staining, and the specific enzyme activity was determined by Baginski assay (Baginski et al., 1967). Both the solubilized *samples A* and *B* were pipetted into small aliquots and stored at − 80 °C.

2.3. Preparation of LCPs

LCPs without protein were prepared by mixing the appropriate amount of molten monoolein (MO) and buffered solutions of 50 mM TRIS/HCl pH 7.4 with 1.12 mg ml^{-1} $C_{12}E_8$ (for *sample A*) or ISE with 0.08 mg ml^{-1} SDS (for *sample B*) at room temperature in small glass vials. The ratio of components was chosen on the basis of the phase diagrams for the MO/water system (Qiu and Caffrey, 2000). The composition of the non-doped LCPs was 60.2/39.8 (w/w) % for MO/buffer. LCPs with incorporated NKA were prepared similarly as described above, first NKA *sample A* or *B* was diluted in buffer solution and mixed with the appropriate amount of molten MO. The final composition of the NKA-doped LCPs was 60/0.2/39.8 (w/w) % for MO/NKA/buffer. Samples were stabilized for at least 48 h to obtain transparent, viscous, and homogenous LCPs. Samples were stored in tightly closed vials at room temperature in the dark. Their stability was confirmed by macroscopic observation of the samples and by small-angle X-ray scattering (SAXS) measurements.

2.4. SAXS analysis

The phase identity and structural parameters of the lipidic samples were determined by SAXS. The experiments were carried out with a Bruker Nanostar system equipped with a Vantec-2000 area detector using CuKα radiation (λ = 1.54 Å). LCP formulations were injected into 1.5-mm diameter quartz capillaries sealed with epoxy glue (UHU). The temperature in the sample cell was kept at 22 °C and was regulated by a Peltier element, while the scattered intensity was collected over 20 min. The scattering intensities I(q) were represented as a function of the magnitude of the scattering vector $q = (4\pi/\lambda)\sin(\theta)$, where 2θ is the scattering angle and λ is the wavelength of the incoming X-ray beam. The 2D images were integrated to produce 1D plots representing the scattering intensity I *vs.* q, called scattering profiles. The lattice parameter (a) for Pn3m LCP was calculated using the following equation:

$$a = \frac{2\pi}{q}\sqrt{h^2 + k^2 + l^2} \quad (1)$$

, where q is the scattering vector, and *h*, *k*, and *l* are the Miller indices of the Bragg peaks.

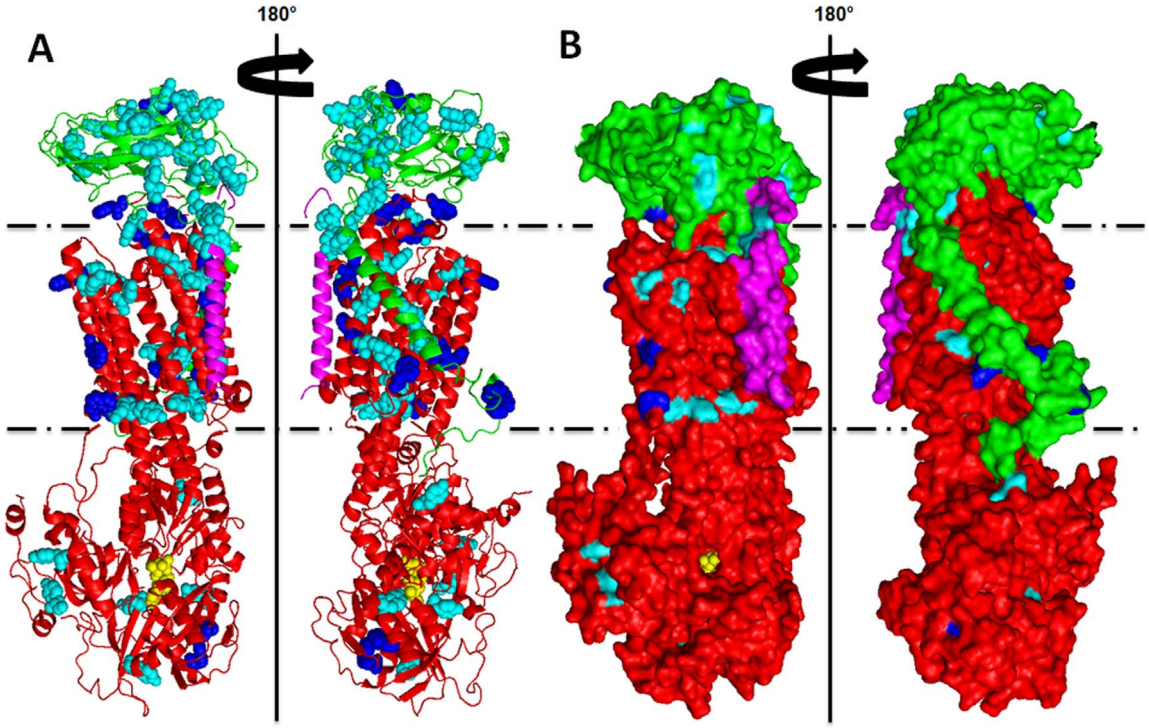

Scheme 1. (A) Molecular model of Na^+/K^+ ATPase (3WGV) with highlighted α (red), β (green), and γ (magenta) subunits. **(B)** Electroactive amino acid residues on surface of protein: Tyr (cyan), Trp (blue), and ADP bound (yellow). The left and right hand images are mutually rotated by 180° along the vertical axis for each panel. The horizontal lines approximately delineate the membrane. (For interpretation of the references to color in this figure legend, the reader is referred to the web version of this article).

To determine the aqueous channel radius, the water volume fraction was estimated using the following Eq. (2) (Turner et al., 1992)

$$\varphi_{water} = \frac{c_{water}}{c_{water} + (1-c_{water})\frac{\rho_{water}}{\rho_{lipid}}} \quad (2)$$

where φ_{water} is the water volume fraction, c_{water} is the water weight fraction, ρ_{water} is the density of water = 0.997 g ml^{-1}, and ρ_{lipid} is the density of the lipid (ρMO = 0.942 g ml^{-1}).

Next, the lipid volume fraction was estimated from Eq. (3):

$$\varphi_{lipid} = 1 - \varphi_{water} \quad (3)$$

Lipid length was obtained by solving Eq. (4)

$$\varphi_{lipid} = 2A_0\left(\frac{l}{a}\right) + \frac{4}{3}\pi\chi\left(\frac{l}{a}\right)^3 \quad (4)$$

, where l is the lipid chain length/monolayer thickness, a is the lattice parameter of the corresponding phase, A_0 is the Euler–Poincaré characteristic, χ is the ratio of the area of the minimal surface in a unit cell to (unit cell volume)$^{2/3}$. Finally, the aqueous channel radius was obtained from Eq. (5):

$$r_w = \left(-\frac{A_0}{2\pi\chi}\right)^{1/2}a - l \quad (5)$$

For the *Pn*3*m* phase, $A_0 = 1.919$, $\chi = -2$.

2.5. Enzyme activity measurement

The measurement of the specific activity of NKA was performed in a buffer designed to promote activity containing 30 mM imidazole, 130 mM NaCl, 20 mM KCl, 4 mM $MgCl_2$, and 3 mM ATP, in the presence or absence of 1 mM ouabain, at pH 7.4. After the incubation of NKA with 48 µl of buffer, the enzyme activity was stopped by the addition of 75 µl of reaction mixture containing 0.16 mM ascorbic acid, 2.4% (v/v) acetic acid, 1.3% (v/v) SDS, and 0.5% (w/v) $(NH_4)_6Mo_7O_{24}$, ammonium molybdate. Ammonium phosphomolybdate complex development was stopped by adding 125 µl of a mixture containing 0.9% (w/v) bismuth citrate, 0.9% (w/v) sodium citrate and 3.7% (v/v) HCl. The amount of ammonium phosphomolybdate complex was determined at 710 nm by spectrophotometric analysis (Baginski et al., 1967) or by cyclic and square-wave voltammetry. Ouabain-sensitive NKA activity was calculated as the difference in the P_i content in nmol P_i mg^{-1} protein min^{-1} between media with and without the inhibitor. The calibration line was obtained using KH_2PO_4 solutions over the concentration range 0–25 nM. Under these conditions, NKA should presumably be found in the E1 conformation (Scheme 1) (Nyblom et al., 2013).

2.6. Electrode modification procedure

A glassy carbon electrode (GCE, BASi, 3 mm diameter, or GCE, Bio-Logic SAS, 1 mm diameter) was weighed before and after immobilization of the LCPs to ensure that approximately the same amount of cubic phase was placed on the electrode surface. The immobilization procedure was performed by simple immersion of the electrode surface into the LCP matrix to fully cover the electrode surface. The amount of cubic phase immobilized on the electrode surface was *ca.* 0.7 mg per mm^2. After the immobilization step, the modified electrode was immersed in the supporting electrolyte solution 15 min before each experiment. This time was needed for equilibration of the cubic phase.

2.7. Electrochemical measurements

All electrochemical measurements were performed at room temperature with a CHI bipotentiostat and a three-electrode arrangement with an Ag/AgCl (3 M KCl) electrode as the reference and platinum foil as the auxiliary electrode. Cyclic voltammetry (CV) and square-wave voltammetry (SWV) experiments were carried out using a GCE (BASi, 3 mm diameter, or GCE, Bio-Logic SAS, 1 mm diameter). Prior to each experiment, the GCE was polished mechanically with 1.0, 0.3, and 0.05 µm alumina powder on a Buehler polishing cloth to produce a mirror-like surface. The electrodes were subsequently sonicated to remove adhered alumina particles, rinsed with water, and left to dry.

2.8. Statistical analysis

Results were expressed as means ± standard deviation (SD) based on three independent measurements ($n = 3$). Statistical analysis was carried out using Statistica software (version 12.0) by one-way ANOVA and Student's *t*-test.

3. Result and discussion

3.1. SAXS measurement of monoolein (MO) based LCPs with incorporated NKA

A number of factors can affect the behaviour of the MO-water system. The incorporation of any additives (proteins, detergents) into the MO-based LCP may have a significant effect on the phase behaviour. Misquitta and Caffrey, 2003, reported the effect of non-ionic detergents, the *n*-alkyl-β-D-glucopyranosides, on LCP behaviour. They showed that small amounts of detergent could be introduced to the LCP without significant change in the LCP structure, whereas increasing concentrations of detergent led to the Pn3m *via* Ia3d to lamellar phase transition. Electrolytes can also lead to changes in the lattice parameters. For example, sodium chloride or sodium sulphate have strong hydrating effects, leading to the shrinking of the water channels and resulting in the lattice parameter decreasing. Sodium thiocyanate or sodium iodide have the opposite effect, leading to increased lattice parameters reflecting the swelling of the LCP's water channels (Cherezov et al., 2006; Liu and Caffrey, 2005; Misquitta and Caffrey, 2003).

SAXS was used to determine the effect of the incorporation of NKA on the LCP's symmetry and its structural parameters. SAXS measurements were performed on NKA-doped LCPs with compositions of 60/0.2/39.8 (w/w) % for MO/NKA/buffer. The non-doped LCP systems were prepared from water, TRIS-HCl buffer (for NKA *sample A*) and ISE buffer (for NKA *sample B*), both at pH 7.4. In all the measured systems, the total water/buffer content was held constant at 39.8 (w/w) %. To purify and to achieve the solubility of NKA at room temperature, 0.02% (w/w) of detergent, $C_{12}E_8$ (for *sample A*) or SDS (for *sample B*) was added, in the appropriate buffer. The effect of the NKA and detergents contained in *samples A* and *B* on the LCP properties is shown in Fig. 1.

1D diffraction patterns for the studied LCP formulations showed reflections in the ratios of √2, √3, √4, √6, √8, √9, which are the characteristic reflections for the cubic-Pn3m phase. The symmetry, lattice parameters, lipid length and aqueous channel diameter for MO-based LCPs with and without NKA are listed in Fig. 1C. The effect of the buffers or detergents used on the cubic phase nanostructure was found to be non-significant, some slight differences in the lattice parameters may be caused by differences in hydration. We thus conclude that the introduction of the NKA at the concentration used here does not alter the internal structure of the LCP. It is important to note that the initial structure of LCP-NKA is definitely under control for all operations prior to NKA activity measurement.

At the concentrations of protein used in the present study we did not observe changes in the LCP symmetry and lattice parameter. SAXS measurements were done repeatedly. After electrochemical experiment LCP was still transparent indicating cubic phase structure. From the literature data it is known also that changing in the pH has extremely small effect on the MO based LCP structure.

3.2. Electrode behaviour of NKA

The electrochemical oxidation of NKA incorporated into LCPs was studied by CV and SWV. The voltammograms were recorded using cubic-phase modified GCE in acetate buffer (pH 4.8) solutions. In the CV experiments using electrodes covered with LCPs containing NKA, two well-resolved oxidation peaks were found: peak Y, at a potential $E_{pY} = +0.5$ V, and peak W, at a potential $E_{pW} = +0.7$ V (Fig. 2). The oxidation peaks Y and W are associated with oxidation on the Tyr and Trp located on the surface of the parts of NKA exposed to the electrode surface. NKA contains 48 Tyr and 16 Trp residues in total, of which 7 Tyr and 5 Trp residues are located in the transmembrane part or at the water/lipid interface region, and 21 Tyr and 4 Trp residues are located in the β-subunit. The cytoplasmic part contains only 8 Tyr and 6 Trp residues (Zatloukalová et al., 2012).

In the SW voltammograms, E_{pY} was + 0.4 V and E_{pW} was + 0.6 V (Fig. 2) ascribed to the anodic reaction of Tyr (Y) and Trp (W) residues located on the surface of the protein (highlighted in Scheme 1) (Zatloukalová et al., 2012). The measurements with butyrylcholine modified GCE, show that the anodic reaction of Tyr is a one-electron, one-proton reaction, while the oxidation of Trp proceeds with the exchange of two electrons and two protons (Jin and Lin, 2004). Current response increases with the concentration of incorporated NKA, as can be observed either on CV or SWV (Fig. 2). The data describing the anodic behaviour of NKA investigated in proteoliposomes (Vacek et al., 2016) and NKA cytoplasmic loop C45 (Zatloukalová et al., 2012) are in good agreement with our LCP results.

3.3. Activity of NKA incorporated in LCPs

After the SAXS determination of the LCP's properties and electrochemical *in situ* verification of NKA's presence in LCP matrices, the NKA activity in the LCPs was evaluated by spectrophotometry *ex situ*. For this purpose, NKA *sample A* embedded into LCP was incubated with all the components that are required for the ATP-hydrolysing reaction in buffered solution. The ATP-hydrolysing catalytic reaction of NKA proceeds in the presence of sodium, potassium and magnesium ions, where NKA was able to convert ATP to ADP. Free phosphate (P_i) was released during this reaction. In the spectrophotometric assay, P_i reacted with ammonium molybdate and reducing agents in the acidified solution to form the blue α-Keggin anion, which was detected spectrophotometrically at a wavelength of 710 nm (Baginski et al., 1967; Kolliopoulos et al., 2015):

$$7PO_4^{3-} + 12Mo_7O_{24}^{6-} + 72H^+ \rightarrow 7PMo_{12}O_{40}^{3-} + 36H_2O$$

To determine the NKA activity, a calibration curve was constructed that was based on the above reaction of P_i in the presence of $(NH_4)_6Mo_7O_{24}$ and ascorbic acid. The activity of NKA embedded into the LCPs was found to be 4.62 nmol Pi $mg^{-1}$of protein min^{-1} after 6 days of hosting the enzyme in LCPs (Fig. 3A). To eliminate nonspecific interactions and the contribution of the background, the absorbance of LCP samples without incorporated enzyme was determined under the same conditions.

The spectrophotometric method, however, suffers from refractive index errors and turbidity interferences. Therefore, electrochemical methods were also utilized for phosphate monitoring in biosensors (Akyilmaz and Yorganci, 2007; Ejhieh and Masoudipour, 2010; Gilbert et al., 2011).

The ammonium phosphomolybdate complex generated as the result of the ATP-hydrolysing reaction was subsequently determined by voltammetry using an unmodified GCE under the same conditions as described above. The calibration curve was prepared using KH_2PO_4 and ammonium molybdate in the buffer (pH 7.4) containing 30 mM imidazole, 130 mM NaCl, 20 mM KCl, 4 mM $MgCl_2$ and 3 mM ATP. In the presence of reducing agent, ascorbic acid, the oxidation of ammonium phosphomolybdate complex under acidic conditions was recorded. SW voltammograms shown in Fig. 3B exhibit two oxidation peaks: A_1 at potential, $E_{p1} = +0.24$ V and A_2 at potential, $E_{p2} = +0.38$ V. The oxidation processes were accompanied by reduction counterparts, indicating reversibility of the electrode processes. The linear dependence of peak current A_1 on the concentration of KH_2PO_4 (Fig. 3B) proves that SWV enables the determination of phosphate and is suitable for monitoring phosphate release. Based on the previously reported results, we ascribe the first oxidation peak A_1 to the oxidation of molybdenum(II)

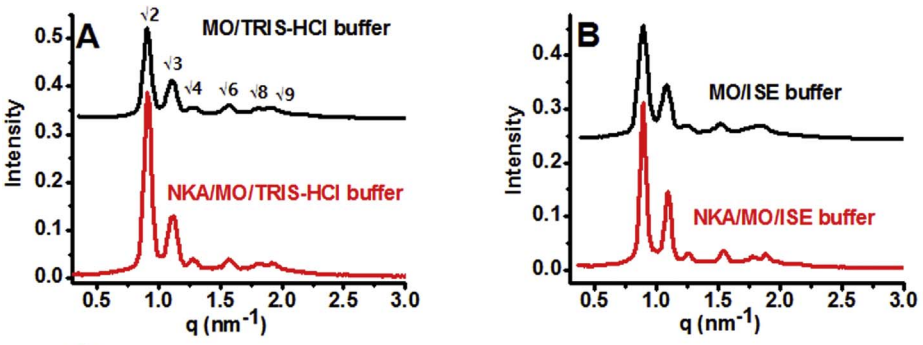

Fig. 1. SAXS profile of monoolein-based lipid cubic phase (LCP) without (black lines) or with (red lines) incorporated NKA (0.2% w/w). **(A)** commercial NKA *sample A* in TRIS/HCl (pH 7.4) and **(B)** isolated NKA *sample B* in ISE buffer (pH 7.4). **(C)** Symmetry, lattice parameters, lipid length and aqueous channel diameters for monoolein (MO) – based lipidic cubic phases (LCPs) with or without incorporated Na^+/K^+-ATPase (NKA). The differences between means (in each column) were considered to be statistically non-significant ($p < 0.05$).

C

LCPs composition	Phase symmetry	Lattice parameter a (nm)	Lipid lengh l (nm)	Channel width d (nm)
MO + water 60.2/39.8 (w/w) %	Pn3m	10.4±0.10	1.77±0.02	4.5±0.00
MO + 50 mM TRIS/HCl (pH 7.4) 60.2/39.8 (w/w) %	Pn3m	9.8±0.05	1.66±0.05	4.4±0.00
MO + 50 mM TRIS/HCl (pH 7.4) with $C_{12}E_8$ detergent 60.2/39.8 (w/w) %	Pn3m	9.9±0.05	1.68±0.01	4.4±0.05
MO + 50 mM TRIS/HCl (pH 7.4) with $C_{12}E_8$ detergent + NKA 60/0.2/39.8 (w/w) %	Pn3m	9.9±0.10	1.68±0.02	4.4±0.05
MO + ISE buffer with SDS (pH 7.4) 60.2/39.8 (w/w) %	Pn3m	10.3±0.00	1.73±0.00	4.5±0.00
MO + ISE buffer pH (7.4) with SDS+ NKA 60/0.2/39.8 (w/w) %	Pn3m	10.2±0.05	1.75±0.00	4.5±0.00

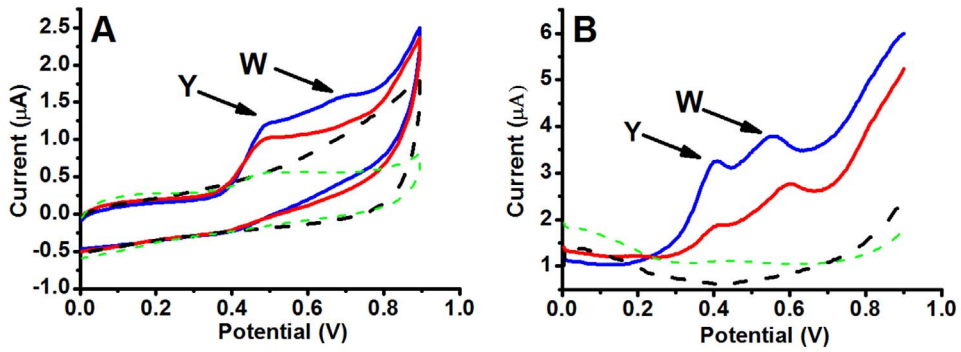

Fig. 2. CV **(A)** and SWV **(B)** curves recorded with GCE modified with lipidic cubic phases (LPC) with or without incorporated Na^+/K^+-ATPase (NKA *sample A*), Y = oxidation peak of Tyr, W = oxidation peak of Trp residues. LCPs with incorporated NKA (0.2% w/w, blue lines or 0.1% w/w, red lines). Green dashed lines: LCPs without NKA. Black dashed lines: supporting electrolyte acetate buffer (pH 4.8). CV scan rate: 50 mV s^{-1}. SWV amplitude: 25 mV, frequency: 20 Hz, E_{init} = 0 V.

to molybdenum(IV) and the following peak A_2 to the oxidation of molybdenum(IV) to molybdenum(VI) complexes (Kolliopoulos et al., 2015).

The reducing agent, ascorbic acid, can be replaced with electrochemical generation of the reduced forms of the phosphomolybdate complex. In this case, electroreduction of phosphomolybdate complex was performed on the GCE and studied by CV and SWV. Two reduction peaks and their oxidation counterparts can be seen in the voltammograms (Fig. S1 in Supporting information). Both pairs of peaks correspond with reduction/oxidation of the phosphomolybdate complex, as reported previously (Kolliopoulos et al., 2015; Zezza et al., 2012).

After optimization of the voltammetric approach, we studied the activity of NKA incorporated into LCPs using an unmodified GCE. A known amount of NKA incorporated into LCPs and non-modified LCPs were placed in small vials to which pure buffer or buffer with ouabain inhibitor were added. After the incubation time, the reaction was stopped and the solution was transferred to the electrochemical cell. The SW voltammogram showed two oxidation peaks, at potentials E_{p1} = + 0.24 V and E_{p2} = + 0.38 V (Fig. 3C). The oxidation of the ammonium phosphomolybdate complex in the presence of reducing agent took place in two successive steps under these conditions. SW voltammograms of LCPs without and with the incorporated protein in the presence of inhibitor, 1 mM ouabain were done under the same conditions. Based on the calibration curve of the ammonium phosphomolybdate complex, the ouabain-sensitive NKA activity in LCPs was found to be 3.88 nmol Pi mg^{-1} protein min^{-1} after 6 days of hosting the enzyme in LCPs.

3.4. NKA activity in immobilized LCP matrix

The high viscosity of LCPs enables their application on solid substrates such as electrodes leading to a cubic phase film-modified electrode. This approach minimizes the amount of enzyme sample necessary for electroanalysis and increases its stability. SW voltammograms (Fig. 4A) revealed the presence of the two oxidation peaks (Ep_1 = + 0.21 V and Ep_2 = + 0.32 V) corresponding to the oxidation of the phosphomolybdate complex on the GCE. Both oxidation peaks were slightly shifted to less positive potentials compared to those recorded using the bare electrode. The potential shift of the first and second oxidation peaks was around 30 mV and 60 mV, respectively. The shift could be connected with the immediate environment of specific interactions of large Keggin type anions with hydrophilic groups of the

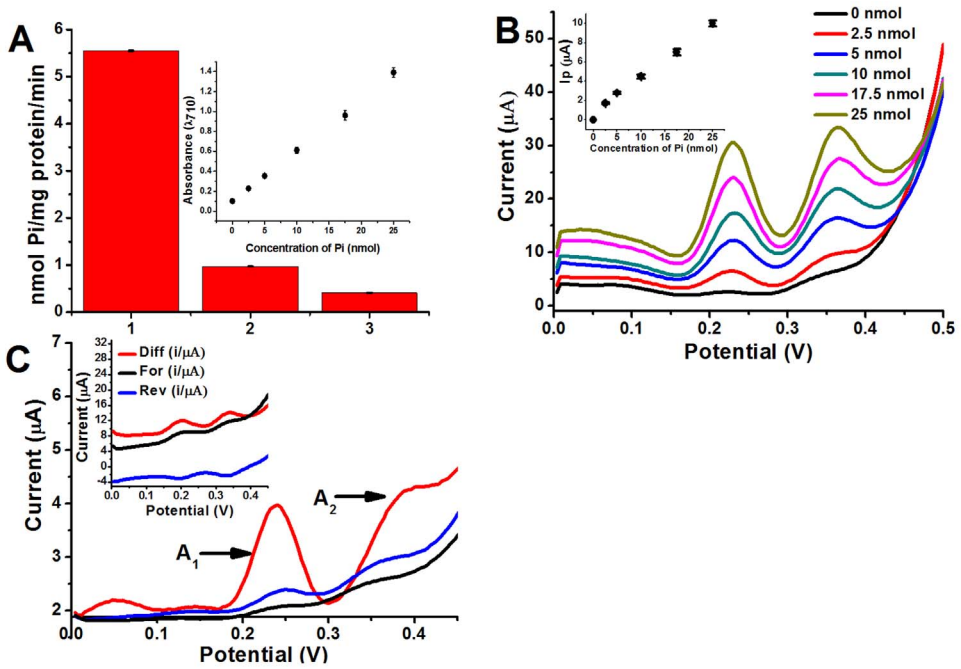

Fig. 3. (A) Spectrophotometric analysis of ATP-hydrolysing activity of Na^+/K^+-ATPase (NKA) incorporated into LCPs measured at 710 nm. Activity of LCP **(1)** with NKA; **(2)** with NKA in presence of 1 mM inhibitor ouabain; **(3)** without NKA. **Inset:** Calibration curve: P_i in presence of 7 mM $(NH_4)_6Mo_7O_{24}$ and 0.16 mM ascorbic acid. **(B)** SWV records for different concentrations of ammonium phosphomolybdate complex recorded using unmodified GCE. **(C)** SWV curves reflecting NKA activity incorporated into LCP using GCE. Red line: LCPs with incorporated NKA, blue line: LCP with incorporated NKA in presence of ouabain inhibitor, black line: LCP alone. **Inset:** SWV forward, backward and net current. Supporting electrolyte: buffer containing 30 mM imidazole, 130 mM NaCl, 20 mM KCl, 4 mM $MgCl_2$ and 3 mM ATP in presence of 0.16 mM ascorbic acid and 7 mM ammonium molybdate (pH 2). Amplitude: 25 mV, frequency: 80 Hz. NKA *sample A* was used.

lipids. However, more experiments will have to be done to confirm this hypothesis.

A calibration curve where KH_2PO_4 reacts with ammonium molybdate was prepared using the GCE modified with LCPs (Fig. 4B). The NKA activity in LCPs was found to be 4.02 nmol Pi mg^{-1} protein min^{-1} after 6 days of hosting the enzyme in LCPs. The activity of NKA incorporated into LCPs was also studied in the presence of the inhibitor, ouabain. The oxidation peaks A_1 and A_2 decreased in the presence of ouabain (Fig. 4A).

3.5. Long-term stability of the LCP-NKA films

Finally, we studied the LCP-hosted NKA activity of *sample A* and *B* in LCPs for several days, and the results were compared with the activities of these proteins in solubilized form (Fig. 5). The activity of solubilized *samples A* and *B* decreased dramatically after 4 days and 1 day, respectively, when left at room temperature. On the sixth day, both NKA samples had less than 30% of their initial activity. It is known that proteins which have cysteine residues in their structure undergo oxidation in the presence of molecular oxygen. To prevent NKA oxidation, reducing agents such as dithiotreitol (DTT) or tris(2-carboxyethyl) phosphine (TCEP) can be used. The activity of solubilized NKA in the presence of 1 mM DTT and 1 mM TCEP was measured over 7 days (Fig. 5), however no improvement in the stability of the solubilized protein was found.

The NKA-LCP activity was determined spectrophotometrically *ex situ* and using SWV with immobilized LCPs containing NKA samples. If we compare the activity of *sample B* with the commercially available one (*sample A*), the isolated NKA was able to convert more than 100 nmol Pi mg^{-1} protein min^{-1} (in good agreement with (Klodos et al., 2002)), while the commercially available NKA converted only 7.7 nmol Pi mg^{-1} protein min^{-1} under the same experimental conditions (Figs. 5A and 5B). Compared to the solubilized samples of NKA, the activities of NKA incorporated into LCPs were significantly higher and the proteins were more stable in the lipidic environment. The NKA activities remained unchanged after one week, while after 14 days more than 60% of the protein activity was retained. The activity of NKA embedded into LCP was near to 300 nmol Pi mg^{-1} min^{-1} and was comparable to the activity of NKA reconstituted in unilamellar DPPC/DPPE liposomes under very similar experimental conditions (Vacek et al., 2016).

4. Conclusions

The membrane protein NKA-LCP system was characterized by SAXS and the phase's structural parameters were determined as a double-diamond (Pn3m) cubic phase. The ouabain-sensitive NKA activity of the encapsulated enzyme in LCPs was investigated in detail. The ATP-hydrolysing activity of NKA incorporated into LCPs was 4.62 nmol Pi mg^{-1} protein min^{-1}. The activity was 3.88 nmol Pi mg^{-1} protein

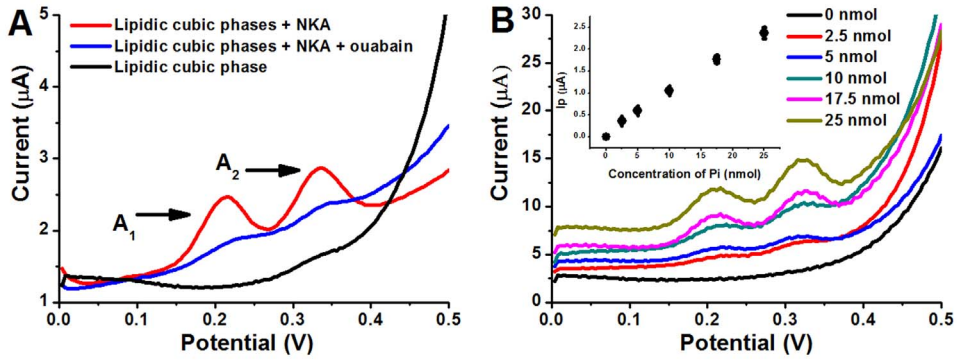

Fig. 4. (A) SWV reflecting Na^+/K^+-ATPase activity incorporated into LCP after immobilization onto GCE surface. **(B)** SWV for increasing concentration of ammonium phosphomolybdate complex recorded using LCP-modified GCE. Supporting electrolyte: buffer containing 30 mM imidazole, 130 mM NaCl, 20 mM KCl, 4 mM $MgCl_2$ and 3 mM ATP in the presence of 0.16 mM ascorbic acid and 7 mM ammonium molybdate (pH 2). Amplitude: 25 mV, frequency: 80 Hz. NKA *sample A* was used.

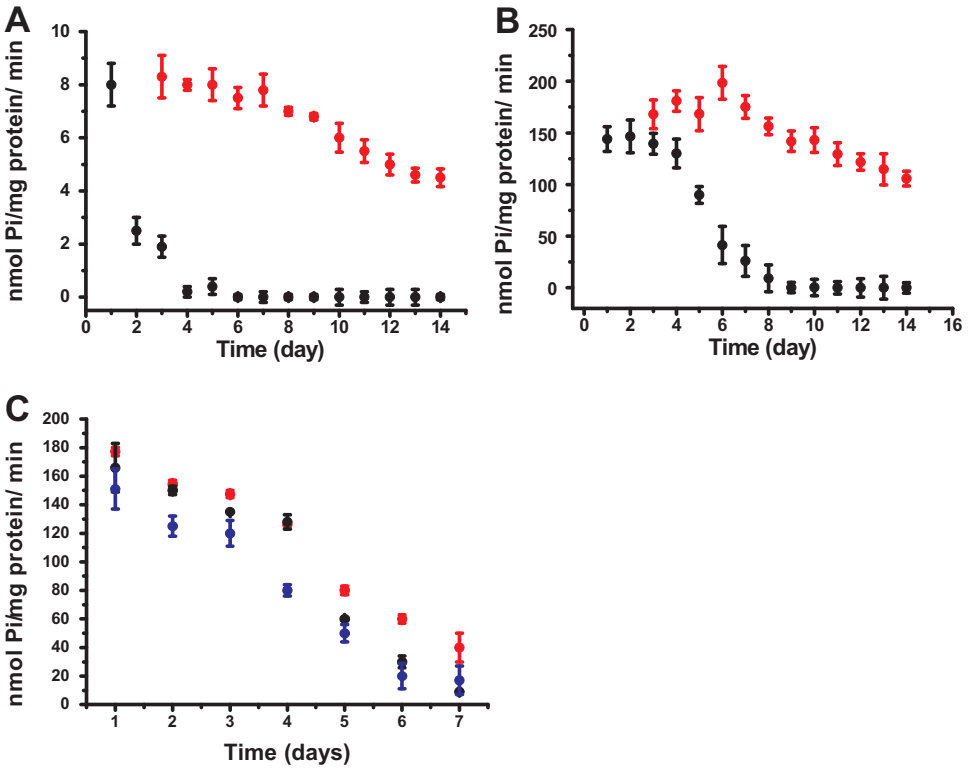

Fig. 5. Ouabain-sensitive activity of **(A)** commercially available (*sample A*) and **(B)** isolated (*sample B*) NKA measured by spectrophotometry at 710 nm over 14 days. Activity of NKA in LCP (0.2% w/w) (red circles) and NKA solubilized (black circles). **(C)** Activity of solubilized NKA: red circles, in presence of DTT: black circles, of TCEP: blue circles. Solution: activity buffer containing 30 mM imidazole, 130 mM NaCl, 20 mM KCl, 4 mM $MgCl_2$, and 3 mM ATP. (For interpretation of the references to color in this figure legend, the reader is referred to the web version of this article).

min^{-1} as determined by SWV after 6 days based on the calibration curve obtained with KH_2PO_4. Thus, the enzyme electrode prepared was sensitive to nmol levels of P_i, reflecting its ATP-hydrolysing activity. Due to the unique properties of the lipidic cubic phases: their biocompatibility and stability in contact with water, these hosting materials provide a novel useful platform for studies of transmembrane proteins activities and functions. This matrix proved to be convenient for work with NKA, since it was shown to retain the activity of the encapsulated enzyme for a long time. The NKAs activity remained unchanged for a week, while after 14 days more than 60% of the enzyme activity was retained. The results obtained should be easily transferred to the other ATP-hydrolysing membrane proteins. The new application of LCP described in this study could also be important for the development of other membrane protein-based electrochemical sensors.

Acknowledgements

This work was supported by the Swiss National Science Foundation (Sinergia Project no. CRSII2_154451/1), by the Czech Science Foundation (Project no. 14-08032S), and by the institutional financial support of Palacky University (Project IGA_LF_2017_011). The authors are indebted to Mr. Ben Watson-Jones MEng for language correction.

Appendix A. Supporting information

Supplementary data associated with this article can be found in the online version at http://dx.doi.org/10.1016/j.bios.2017.09.036.

References

Akyilmaz, E., Yorganci, E., 2007. Electrochim. Acta 52, 7972–7977.
Angelov, B., Angelova, A., Ollivon, M., Bourgaux, C., Campitelli, A., 2003. J. Am. Chem. Soc. 125, 7188–7189.
Baginski, E.S., Foà, P.P., Zak, B., 1967. Clin. Chem. 13, 326–332.
Bartolommei, G., Moncelli, M.R., Tadini-Buoninsegni, F., 2013. PLoS One 8, e58615.
Benabdelhak, H., Schmitt, L., Horn, C., Jumel, K., Blight, M.A., Holland, I.B., 2005. Biochem. J. 386, 489–495.
Boyd, B.J., Whittaker, D.V., Khoo, S.-M., Davey, G., 2006. Int. J. Pharm. 309, 218–226.
Bradford, M.M., 1976. Anal. Biochem. 72, 248–254.
Caffrey, M., 2015. Acta Crystallogr. Sect. F: Struct. Biol. Commun. 71, 3–18.
Cherezov, V., Clogston, J., Papiz, M.Z., Caffrey, M., 2006. J. Mol. Biol. 357, 1605–1618.
Dalla, S., Swarts, H.G.P., Koenderink, J.B., Dobler, S., 2013. Insect Biochem. Mol. Biol. 43, 1109–1115.
Ejhieh, A.N., Masoudipour, N., 2010. Anal. Chim. Acta 658, 68–74.
Ferrandi, M., Tripodi, G., Salardi, S., Florio, M., Modica, R., Barassi, P., Parenti, P., Shainskaya, A., Karlish, S., Bianchi, G., Ferrari, P., 1996. Hypertension 28, 1018–1025.
Fong, W.-K., Negrini, R., Vallooran, J.J., Mezzenga, R., Boyd, B.J., 2016. J. Colloid Interface Sci. 484, 320–339.
Geering, K., 2001. J. Bioenergy Biomembr. 33, 425–438.
Gilbert, L., Jenkins, A.T.A., Browning, S., Hart, J.P., 2011. Sens. Actuators B Chem. 160, 1322–1327.
Jin, G.-P., Lin, X.-Q., 2004. Electrochem. Commun. 6, 454–460.
Johansson, M., Jansson, T., Powell, T.L., 2000. Am. J. Physiol. Integr. Comp. Physiol. 279, R287–R294.
Juel, C., Nordsborg, N.B., Bangsbo, J., 2013. Am. J. Physiol. Integr. Comp. Physiol. 304, R1161–R1165.
Kaplan, J.H., 2002. Annu. Rev. Biochem. 71, 511–535.
Katona, G., Andréasson, U., Landau, E.M., Andréasson, L.-E., Neutze, R., 2003. J. Mol. Biol. 331, 681–692.
Klodos, I., Esmann, M., Post, R.L., 2002. Kidney Int. 62, 2097–2100.
Kolliopoulos, A.V., Kampouris, D.K., Banks, C.E., 2015. Anal. Chem. 87, 4269–4274.
Kulkarni, C.V., Wachter, W., Iglesias-Salto, G., Engelskirchen, S., Ahualli, S., 2011. Phys. Chem. Chem. Phys. 13, 3004–3021.
Landau, E.M., Luisi, P.L., 1993. J. Am. Chem. Soc. 115, 2102–2106.
Landau, E.M., Rosenbusch, J.P., 1996. Proc. Natl. Acad. Sci. USA 93, 14532–14535.
Li, D., Caffrey, M., 2011. Proc. Natl. Acad. Sci. USA 108, 8639–8644.
Liu, W., Caffrey, M., 2005. J. Struct. Biol. 150, 23–40.
Luzzati, V., Tardieu, A., Gulik-Krzywicki, T., Rivas, E., Reiss-Husson, F., 1968. Nature 220, 485–488.
Misquitta, Y., Caffrey, M., 2003. Biophys. J. 85, 3084–3096.
Nazaruk, E., Bilewicz, R., Lindblom, G., Lindholm-Sethson, B., 2008. Anal. Bioanal. Chem. 391, 1569–1578.
Nazaruk, E., Landau, E.M., Bilewicz, R., 2014. Electrochim. Acta 140, 96–100.
Nazaruk, E., Miszta, P., Filipek, S., Górecka, E., Landau, E.M., Bilewicz, R., 2015. Langmuir 31, 12753–12761.
Nyblom, M., Poulsen, H., Gourdon, P., Reinhard, L., Andersson, M., Lindahl, E., Fedosova, N., Nissen, P., 2013. Science 342, 123–127.
Qiu, H., Caffrey, M., 2000. Biomaterials 21, 223–234.
Razumas, V., Kanapienienė, J., Nylander, T., Engström, S., Larsson, K., 1994. Anal. Chim. Acta 289, 155–162.
Santos, J.S., Asmar-Rovira, G.A., Han, G.W., Liu, W., Syeda, R., Cherezov, V., Baker, K.A., Stevens, R.C., Montal, M., 2012. J. Biol. Chem. 287, 43063–43070.
Sarkadi, B., Price, E.M., Boucher, R.C., Germann, U.A., Scarborough, G.A., 1992. J. Biol. Chem. 267, 4854–4858.
Tiefenbrunn, T., Liu, W., Chen, Y., Katritch, V., Stout, C.D., Fee, J.A., Cherezov, V., 2011.

PLoS One 6, e22348.
Toyoshima, C., Kanai, R., Cornelius, F., 2011. Structure 19, 1732–1738.
Turner, D.C., Wang, Z.-G., Gruner, S.M., Mannock, D.A., McElhaney, R.N., 1992. J. Phys. II 2, 2039–2063.
Vacek, J., Zatloukalova, M., Geleticova, J., Kubala, M., Modriansky, M., Fekete, L., Masek, J., Hubatka, F., Turanek, J., 2016. Anal. Chem. 88, 4548–4556.
Van 'T Hag, L., De Campo, L., Garvey, C.J., Feast, G.C., Leung, A.E., Yepuri, N.R., Knott, R., Greaves, T.L., Tran, N., Gras, S.L., Drummond, C.J, Conn, C.E., 2016. J. Phys. Chem. Lett. 7, 2862–2866.
Zabara, A., Negrini, R., Baumann, P., Onaca-Fischer, O., Mezzenga, R., 2014. Chem. Commun. 50, 2642–2645.
Zatloukalová, M., Orolinová, E., Kubala, M., Hrbáč, J., Vacek, J., 2012. Electroanalysis 24, 1758–1765.
Zezza, T.R.C., de Souza Castilho, M., Stradiotto, N.R., 2012. Fuel 95, 15–18.